Resistive Active Balanced Power Divider Design with Touchstone and Kron's Formalism Hybrid Model

Blaise Ravelo [1,2], Fayu Wan [1], Sebastien Lalléchère [3], and Benoit Agnus [4]

[1] Nanjing University of Information Science & Technology, Nanjing, China 210044

[2] Normandy University, UNIROUEN, ESIGELEC, IRSEEM EA 4353
Technopole du Madrillet, Avenue Galilée, BP 10024, F-76801 Saint Etienne du Rouvray, France

[3] UCA, CNRS, SIGMA Clermont, Institut Pascal, France

[4] Av. Blaise Pascal, F-63178 Aubière, WAVE CONCEPTION, 14000 Caen, France
fayu.wan@nuist.edu.cn

Abstract ─ A resistive active power divider (RAPWD) design based on Kron's model is introduced. The three-way RAPWD topology is essentially constructed with a low noise amplifier (LNA) with input and output matching shunt resistances. The RAPWD S-parameter is analytically expressed from the Kron's method hybridized with the LNA touchstone model. The RAPWD synthesis relation is established in function of the expected gain and matching access. The feasibility of the established Kron's method modelling is validated with a proof-of-concept (POC) using the surface mounted monolithic LNA LEE-9+ from mini-circuits. As expected, S-parameters are in good correlation between simulations and computed results from the proposed hybrid method. A relatively flat transmission gain of about 9+/-0.2 dB is realized in the very wide frequency band 0.5 to 4.5 GHz. The broadband tested RAPWD input and output matching and access port isolations are widely better than 10 dB.

Index Terms─ Active microwave circuit, design method, hybrid model, Kron's formalism, Power Divider (PWD), resistive topology, synthesis relations.

I. INTRODUCTION

The power divider (PWD) is one of the key elements and most useful components for the RF/microwave communication system. The PWD RF/microwave function is usually implemented in different front- and back-end architectures as phased array antennas [1-2] and reflectors [3].

The phased array enables to deploy several functions widely used in military and commercial applications as retrodirective antenna system for example based on the Van Atta Array [4]. Various design technologies have been deployed in function of the substrate structures [5] and improving the 3D radiation beam coverage [6]. The phased array architecture is regularly employed in the radar system. It allows to improve the airborne radar performance as can be found in the atmospheric meteorology research [7]. The phased array architecture is also popularly implemented in radio astronomy stations [8-10]. The array antenna is flexible to operate in low-frequency ranges which are potentially useful for the sky radio scanning [8-12]. In addition, the PWD based phased array architectures are potentially integrable in Silicon based radio frequency integrated circuits (RFICs) [13]. So, the phased array elements are potentially designed and implemented in CMOS technology for microwave and millimeter wave applications as 60-GHz [14] and 77-GHz [15] transceivers.

The PWD function can be designed in three- or multiple N-way topologies [16-19]. Several topologies as coplanar waveguide [17], metamaterial [18] and hybrid-expanded coupled line based structures [19] were proposed. However, one of easiest design and implemented PWD are based on the Tee-shape passive circuit. The most popular in RF/microwave engineering is the Wilkinson PWD [20-25]. The Wilkinson PWD has been widely exploited and implemented in coplanar wave guide [22], microstrip [23] and hybrid technology [24] in both narrow- and broad-band frequencies. The Wilkinson PWD can be also used to design more complex microwave function as Balun [25]. Nevertheless, acting as passive devices, Tee- and Wilkinson PWD components suffer about insertion losses.

To tackle this problem, active topologies may constitute an efficient solution in order to compensate the losses. The PWD active topology can be designed similar to multiport power amplifiers [26]. But to cope with the design complexity, simple implementation circuit as resistive and low-noise amplifier (LNA) active multi-way PWD [27-28] is required. However, the analytical

Submitted On: September 26, 2017
Accepted On: January 9, 2018

modelling should require the consideration of the LNA touchstone model. In this paper, we are introducing a simple and efficient computational method of the resistive active PWD topology by using the Kron's formalism as deployed in [29-32]. This typically unfamiliar computational method is based on the tensorial analysis of network (TAN).

The Kron's formalism was initially developed for the modelling of electrical machine. Then, recently, it was extended to the modelling of complex electronic and electrical system electromagnetic compatibility (EMC) [29]. Combined with the transmission line (TL) Branin approach, the extended Kron's formalism has been employed to the modelling of TL based interconnect printed circuit board (PCB) [30-31]. Moreover, the formalism can be potentially used to determine the S-parameter model of PWD. The fast-computational model of quarter wavelength arm Y-shape unequal PWD is communicated recently in conference ACES-China 2017 [32], the structure is shown in Fig. 1. In progress of this Kron's modelling, we may wonder on applicability of the proposed method for the resistive active PWD (RAPWD) using LNA.

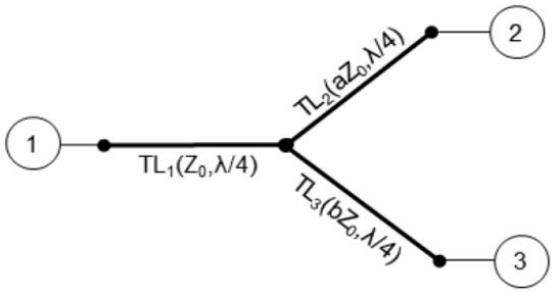

Fig. 1. Y-shape PWD structure [32].

To answer to this technical curiosity, a hybridized model of RAPWD is developed in the present paper. For the better understanding, the paper is organized as follows. Section 2 is dedicated to the proposed circuit computational method. The circuit modelling based on the Kron's formalism and the LNA touchstone model is described. Section 3 addresses the developed hybrid modelling by considering a circuit proof-of-concept (POC). S-parameters simulation results are presented and discussed. Last, Section 4 is the conclusion.

II. THEORY ON THE KRON'S FORMALISM AND TOUCHSTONE HYBRID MODEL OF RESISTIVE ACTIVE POWER DIVIDER

The present section is focused on the hybrid modelling of the three-way PWD. The synoptic of the proposed topology is depicted in Fig. 2. In the present configuration, Port ① is assumed as the input, and Port ② and Port ③ are the outputs.

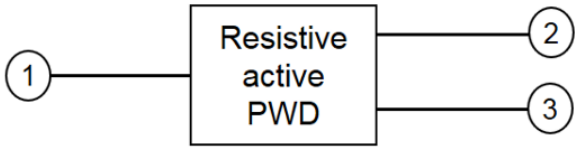

Fig. 2. Synoptic of the RAPWD under study.

The RAPWD is basically implemented by using shut resistances associated with LNA as active elements. Similar to all microwave circuit, in the remainder part of the paper, the proposed theory is established based on the topology S-parameter investigation referenced to the source and load impedance R_0=50 Ω. The calculation principle of the hybrid modelling under study will be illustrated in the coming paragraphs.

A. Resistive and LNA based elementary cell

The elementary cell constituting the proposed RAPWD is sketched in Fig. 3.

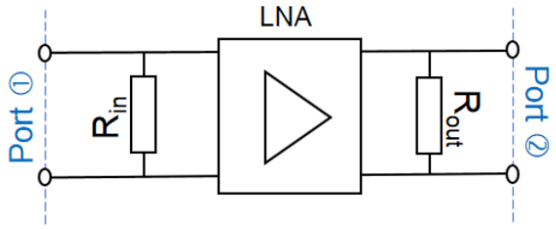

Fig. 3. Considered resistive and active cell constituting the proposed RAPWD.

It consists essentially of an LNA combined with input and output shunt resistances respectively R_{in} and R_{out}. To establish the RAPWD S-parameter, the LNA model is assumed to be provided by the manufacturer in touchstone data. Acting as a two-port S-parameter, the equivalent model can be merely written as:

$$[S_{LNA}(j\omega)]=\begin{bmatrix} S_{LNA_{11}}(j\omega) & S_{LNA_{12}}(j\omega) \\ S_{LNA_{21}}(j\omega) & S_{LNA_{22}}(j\omega) \end{bmatrix}. \quad (1)$$

The LNA is supposed as a unilateral RF/microwave component. Furthermore, it is characterized the input and output matching level equal to S_{LNA11}=S_{LNA22}=r. Meanwhile, the LNA can be represented by the matrix:

$$[S_{LNA}(j\omega)]=\begin{bmatrix} r(j\omega) & 0 \\ t(j\omega) & r(j\omega) \end{bmatrix}. \quad (2)$$

Based on the S-to-Z transform, the equivalent Z-matrix is given by:

$$[Z_{LNA}(j\omega)]=\begin{bmatrix} R_0\dfrac{1+r(j\omega)}{1-r(j\omega)} & 0 \\ 2R_0\dfrac{t(j\omega)}{[1-r(j\omega)]^2} & R_0\dfrac{1+r(j\omega)}{1-r(j\omega)} \end{bmatrix}. \quad (3)$$

B. Graph model of the two-way RAPWD

The RAPWD circuit diagram is illustrated in Fig. 3. The LNAs are inserted at the PWD input and output three arms. The resistance R_1 is connected in shunt at the input for controlling the input matching. Similarly, the resistances R_2 and R_3 are connected in shunt at the outputs for controlling the output matching. The intermediate resistance Rm ensures the stability and the LNA interstage matching. Before setting the Kron's formalism, the system must be traduced in graph representation. The graph equivalent topology of the circuit introduced in Fig. 4. This graph is essentially built by the branches and the black box representing the LNA touchstone S-parameter model. The circuit is fed by voltage sources V_1, V_2 and V_3 respectively connected at Port ①, Port ② and Port ③. It induces the branch currents I_1, I_2 and I_3. The LNA input and output voltages V_α and fictive currents I_α with $\alpha=\{a, b, \dots, i\}$ are indicated in this circuit for mesh law elaboration.

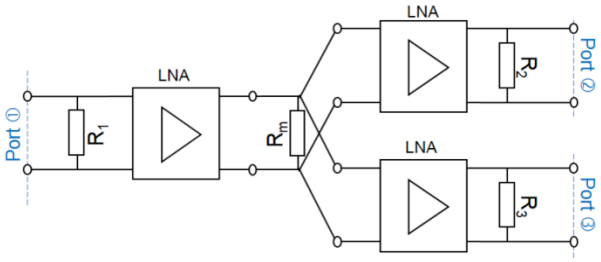

Fig. 4. Circuit topology of the RAPWD.

To construct a symmetrical or balanced PWD, we just have to generate $S_{21}=S_{31}$ and $S_{22}=S_{33}$. This condition can be achieved by implementing same arms at the PWD output branches. In other word, same output shunt resistances $R_2=R_3$ must be used. This idea guarantees the symmetry between the PWD output arms. Consequently, the overall three-port device S-parameter can be determined with the S-parameter of two port system by taking $S_{23}=S_{32}=0$ in addition to the equality $S_{21}=S_{31}$ and $S_{22}=S_{33}$. In this case, the graph introduced in Fig. 5 can be reduced as shown in Fig. 6. The shunt impedance Z_{LNA} represents in the LNA input impedance which is previously given in expression (3).

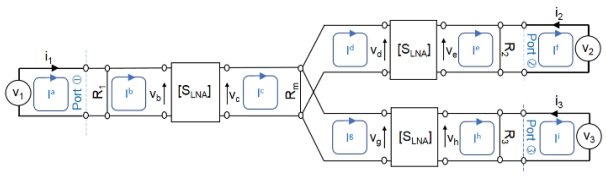

Fig. 5. Equivalent graph topology of the PWD introduced in Fig. 4.

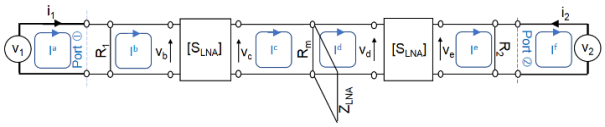

Fig. 6. Reduced equivalent diagram of the graph established in Fig. 5.

C. Discussion on the advantages and the limitation of the RAPWD topology

The combined Kron's formalism and LNA touchstone data hybrid model can be established from the reduced graph proposed in Fig. 6. In order to calculate, the overall system S-parameter, we would start with the three port Z-matrix defined by:

$$\begin{bmatrix} V_1(j\omega) \\ V_2(j\omega) \end{bmatrix} = [Z] \times \begin{bmatrix} I_1(j\omega) \\ I_2(j\omega) \end{bmatrix}, \tag{4}$$

with

$$[Z] = \begin{bmatrix} Z_{11}(j\omega) & Z_{12}(j\omega) \\ Z_{21}(j\omega) & Z_{22}(j\omega) \end{bmatrix}. \tag{5}$$

The analytical expressions governing the system under study can be extracted from the Kron's formalism by assuming that the mesh spaces represented by the current fictive meshes I_α with $\alpha=\{a, b, \dots, i\}$. It implies the following equation system:

$$\begin{cases} V_1(j\omega) = V_b(j\omega) = R_1(I^a(j\omega) - I^b(j\omega)) \\ V_c(j\omega) = V_d(j\omega) = Z_x(I^c(j\omega) - I^d(j\omega)) \\ V_e(j\omega) = V_2(j\omega) = R_2(I^e(j\omega) - I^f(j\omega)) \end{cases}, \tag{6}$$

by denoting the total intermediate impedance as:

$$Z_x = Z_m // Z_{LNA} = \frac{R_0 Z_m (1+r)}{R_0(1+r) + Z_m(1-r)}. \tag{7}$$

In addition to this system, we can consider the LNA model by the transfer matrix:

$$[T(j\omega)] = \begin{bmatrix} T_{11}(j\omega) & T_{12}(j\omega) \\ T_{21}(j\omega) & T_{22}(j\omega) \end{bmatrix}. \tag{8}$$

This transfer matrix is obtained from the LNA touchstone model via the S-to-T transform:

$$\begin{cases} T_{11} = \dfrac{1 + S_{11} - S_{22} - S_{11}S_{22} + S_{12}S_{21}}{2S_{21}} \\ T_{12} = \dfrac{Z_0(1 + S_{11} + S_{22} + S_{11}S_{22} - S_{12}S_{21})}{2S_{21}} \\ T_{21} = \dfrac{1 - S_{11} - S_{22} + S_{11}S_{22} - S_{12}S_{21}}{2S_{21}Z_0} \\ T_{22} = \dfrac{1 - S_{11} + S_{22} + S_{11}S_{22} - S_{12}S_{21}}{2S_{21}} \end{cases}. \tag{9}$$

Therefore, we have the complementary equation system:

$$\begin{cases} V_b(j\omega) = T_{11}(j\omega)V_c(j\omega) + T_{12}(j\omega)I_c(j\omega) \\ I_b(j\omega) = T_{21}(j\omega)V_c(j\omega) + T_{22}(j\omega)I_c(j\omega) \\ V_d(j\omega) = T_{11}(j\omega)V_e(j\omega) + T_{12}(j\omega)I_e(j\omega) \\ I_d(j\omega) = T_{21}(j\omega)V_e(j\omega) + T_{22}(j\omega)I_e(j\omega) \end{cases}. \quad (10)$$

The solution of the combined equations allows to express the unknown voltage in function of the branch currents given by:

$$\begin{cases} V_1(j\omega) = Z_{PWD_{11}}(j\omega)I^b(j\omega) - Z_{PWD_{12}}(j\omega)I^f(j\omega) \\ V_2(j\omega) = Z_{PWD_{21}}(j\omega)I^b(j\omega) - Z_{PWD_{22}}(j\omega)I^f(j\omega) \end{cases}. \quad (11)$$

Finally, the RAPWD S-parameter matrix:

$$\left[S_{PWD}(j\omega)\right] = \begin{bmatrix} S_{PWD_{11}}(j\omega) & S_{PWD_{12}}(j\omega) \\ S_{PWD_{21}}(j\omega) & S_{PWD_{22}}(j\omega) \end{bmatrix}, \quad (12)$$

can be determined from the Z-to-S matrix transform. The expected S-parameter model is given in (13). It can be pointed out that in this ideal case, the PWD isolation losses are zero because of the LNA unilaterality:

$$\begin{cases} S_{PWD_{11}} = \dfrac{2r(j\omega)R_1 - \left[1+r(j\omega)\right]R_0}{2R_1 + \left[1+r(j\omega)\right]R_0} \\ S_{PWD_{12}} = 0 \\ S_{PWD_{21}} = \dfrac{\left\{2r(j\omega)R_2 + \left[1+r(j\omega)\right]R_0\right\}}{\left[1+r(j\omega)\right]\left\{\begin{matrix}\left[1+r(j\omega)\right]R_0 + \\ 3\left[1-r(j\omega)\right]R_m\end{matrix}\right\}} \\ S_{PWD_{22}} = \dfrac{2R_2 + \left[1+r(j\omega)\right]R_0}{2r(j\omega)R_2 + \left[1+r(j\omega)\right]R_0} \end{cases}. \quad (13)$$

D. Proposed RAPWD synthesis relations

The synthesis relations allowing to determine the RAPWD parameters R_1, R_m and R_2 can be extracted from this equation system in function of the specified PWD:

- Input and output matching level m>0 (assumed to be identical).
- And insertion gain g>0.

Doing this, the proposed RAPWD synthesis formulas are determined from the equations:

$$\begin{cases} \left|S_{PWD_{11}}(R_1)\right| = m \\ \left|S_{PWD_{21}}(R_m)\right| = g \\ \left|S_{PWD_{22}}(R_2)\right| = m \end{cases}. \quad (14)$$

As a matter of fact, the formulas enabling to express the RAPWD parameters are written as:

$$R_1 = \begin{cases} \dfrac{R_0(1+r)(1+m)}{2(r-m)} \; if \; r > m \\ \dfrac{R_0(1+r)(1-m)}{2(m+r)} \; if \; r \le m \end{cases}, \quad (15)$$

$$R_2 = \frac{R_0(1+r)(1-m)}{2(m+r)}. \quad (16)$$

$$R_m = \begin{cases} \dfrac{\alpha_1}{3r^3 g(r+2) - \alpha_2 - 3g} \; if \; S_{PWD_{21}} > 0 \\ -2(1+2m)t^2 \\ \dfrac{\alpha_1}{3g + 2(1-2m)t^2 +} \; if \; S_{PWD_{21}} < 0 \\ 3r^3 g(r+2) - \alpha_2 \end{cases}, \quad (17)$$

with

$$\begin{cases} \alpha_1 = R_0 g(r^4 + 4r^3 + 6r^2 + 4r + 1) \\ \alpha_2 = 2m^2 r^2 \end{cases}. \quad (18)$$

III. SIMULATION VALIDATION RESULTS

This section is focused on the validations of the developed hybrid modelling concept. A POC of RAPWD is designed and fabricated following the synthesis approach described in the previous section. The POC modelled computed results are compared with simulations run in the ADS® environment of the electronic circuit designer and simulator.

A. RAPWD POC description

The PWD POC is a three-port active microwave circuit. This POC was designed with the surface mounted monolithic LNA LEE-9+ from mini-circuits. Figure 7 represents the schematic of the POC circuit prototype.

Initially, the RAPWD expected generating transmission gain of about 9 dB and access port reflection coefficients better than 10 dB was synthesized. Therefore, the calculated RAPWD parameters are R_1=R_2=R_3=200 Ω and R_m=62 Ω. The circuit was biased with V_0=5V_{DC} power supply. The designed, fabricated, simulated and measured POC is represented in Figs. 7. The bias circuits are consisted of self-inductance L=75 nH and C_p=100 pF. The DC blocking capacitors are C=100 pF.

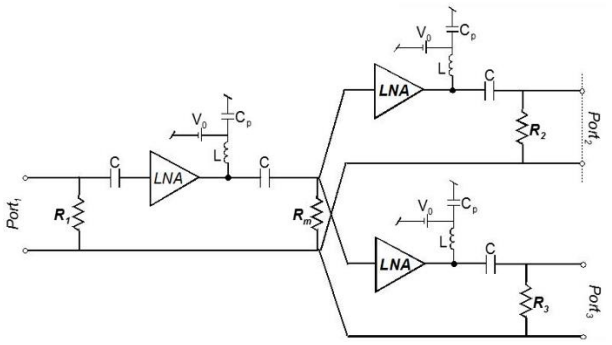

Fig. 7. RAPWD POC simulated circuit design

B. S-parameter results

The validation simulations were performed from 0.5

to 4.5 GHz by using the LNA touchstone model provided by the manufacturer. Figure 8 represents the comparison between the simulated and ideal theory S-parameters obtained from the POC depicted in Fig. 7.

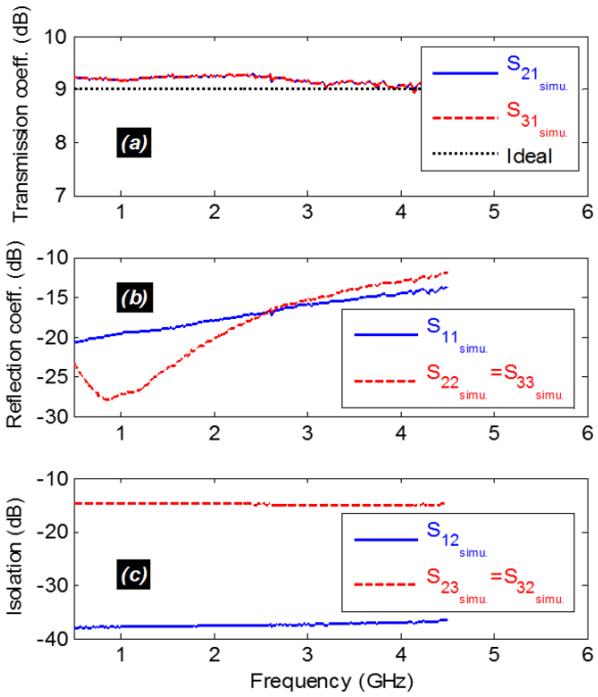

Fig. 8. Comparison of the simulated and ideal theory S-parameters: (a) transmission gains, (b) reflection coefficients, and (c) isolations.

It acts as a very broadband PWD. As seen in Fig. 8 (a), the RAPWD presents a transmission gain with excellent flatness of about 9+/-0.2 dB from 0.5 GHz to 4.5 GHz. Then, as shown in Fig. 8 (c), the isolations are better than 10 dB. The result is very well-correlated to the targeted transmission gain. In addition, as shown in Fig. 8 (b), the three-port access matching is better than 10 dB.

C. Discussion on the advantages and the limitation of the RAPWD topology

The presented RAPWD topology is particularly advantageous in terms of:

- The isolation because of the LNA unilaterality.
- The gain flatness is not easy to achieve for most of passive PWD expected the fully resistive ones. However, with the proposed topology, we have a possibility to generate a very wide bandwidth by choosing the expected LNA.
- The stability which is not, in general, easy to control if the passive PWD to be cascaded with the LNA is not very well matched even out of the operating frequency band.

However, the RAPWD presents drawbacks in matter of:

- The power efficiency because of the shunt resistor which is susceptible to consume and waste energy via Houle effect.
- And the complexity of bias network associated with the DC blocking circuitry.

IV. CONCLUSION

A hybrid modelling methodology of resistive active PWD is investigated. The active topology is mainly consisted of LNA element and shunt resistances. The introduced PWD topology enables to compensate losses and minimize the interbranch isolation in difference with the popular passive PWD topologies. The developed modelling concept is built with the Kron's formalism and the LNA touchstone model. The PWD S-parameter model in function of the LNA S-parameter is established. Then, the synthesis formulas enabling to determine the PWD parameters are expressed. The established theory is validated with resistive active PWD POC. The S-parameter simulation confirms the expected values specified in the synthesis formulas.

It should be emphasized that the proposed RAPWD is advantageous to generate competitive gain flatness, isolation and matching. But it presents some weakness in terms of power efficiency and bias/DC blocking circuitry. In the future, we expect to apply the proposed hybridized Kron's method to more complex active RF/microwave topology by taking into account the power efficiency.

ACKNOWLEDGMENT

The authors address their grateful thanks to Dr. Olivier Maurice for his advice to develop the Kron's formalism based microwave circuit.

This work was supported by NSFC (61601233 and 61750110535). And this work was also partly supported by the FEDER fund from BRIDGE project in Normandy Region, by NSF of Jiangsu (BK20150918), by Defence Research Foundation (6140209050116 ZK53001), by Jiangsu Innovation and Enterprise Group Talents Plan 2015 (SRCB201526), and by PAPD.

REFERENCES

[1] H. A. Wheeler, "Simple relations derived from a phased-array antenna made of an infinite current sheet," *IEEE Trans. AP*, vol. 13, no. 14, pp. 506-514, July 1965.

[2] G. L. Charvat, "Visualization of a phased array antenna system," *Available Online* [2017], https://hackaday.com/2017/01/05/visualization-of-a-phased-array-antenna-system/

[3] B. T. Toland, L. D. Gilger, R. Y. Chan, A. S. Barlevy, and S. J. Hamada, "Deployable phased array of reflectors and method of operation," *Patent US 6268835 B1*, July 2001.

[4] L.Chen, X.-H. Wang, X.-W. Shi, T.-L. Zhang, and

J.-Z. Tong, "Design of a broadband frequency offset van atta array," *PIER Letter*s, vol. 13, pp. 161-171, 2010.

[5] J. B. West and J. C. Mather, "Phased array antenna interconnect having substrate slat structures," *Patent US 7170446 B1*, Jan. 2007.

[6] D. Choudhury, R. Roberts, and U. Karacaoglu, "Wireless antenna array system architecture and methods to achieve 3d beam coverage," *Patent US 20110014878 A1*, Jan. 2011.

[7] E. Loew, J. Salazar, P. S. Tsai, J. Vivekanandan, W. Lee, and V. Chandrasekar, "Architecture overview and system performance of the airborne phased array radar (APAR) for atmospheric research," *Proc. 36rd Conf. on Radar Meteor.*, Breckenrigde, CO, USA, pp. 159-164, 16-20 Sept. 2013.

[8] S. W. Ellingson, "Sensitivity of antenna arrays for long-wavelength radio astronomy," *IEEE Trans. Antennas and Propagation*, vol. 59, no. 6, pp. 1855-1863, June 2011.

[9] G. B. Taylor, S. W. Ellingson, N. E. Kassim, et al., "First light for the first station of the long wavelength array," *J. Astronomical Instrumentation*, vol. 1, no. 1, 1250004, pp. 1-56, 2012.

[10] S. W. Ellingson, T. E. Clarke, A. Cohen, N. E. Kassim, Y. Pihlstrom, L. J. Rickard, and G. B. Taylor, "The long wavelength array," *Proc. IEEE*, vol. 97, no. 8, pp. 1421-1430, Aug. 2009.

[11] M. Harun and S. W. Ellingson, "Design and analysis of low frequency strut-straddling feed arrays for EVLA reflector antennas," *Radio Sci.*, vol. 46, no. 3, RS0M04, pp. 1-12, June 2011.

[12] S. E. Cutchin, J. H. Simonetti, S. W. Ellingson, A. S. Larracuente, and M. J. Kavic, "Constraining the rate of primordial black-hole explosions and extra dimension scale using a low-frequency radio antenna array," *Pub. Astr. Soc. Pacific*, vol. 127, no. 958, pp. 1269-1278, Dec. 2015.

[13] G.-M. Rebeiz and K.-J. Koh, "Silicon RFICs phased arrays," *IEEE Microwave Magazine*, vol. 10, no. 3, pp. 96-103, May 2009.

[14] E. Cohen, M. Ruberto, M. Cohen, O. Degani, S. Ravid, and D. Ritter, "A CMOS bidirectional 32-element phased-array transceiver at 60 GHz with LTCC antenna," *IEEE Trans. MTT*, vol. 61, no. 3, pp. 1359-1375, Mar. 2013.

[15] A. Natarajan, A. Komijani, X. Guan, A. Babakhani, and A. Hajimiri, "A 77-GHz phased-array transceiver with on-chip antennas in silicon: Transmitter and local LO-path phase shifting," *IEEE Journal of Solid-State Circuits*, vol. 41, no. 12, pp. 2807-2819, Dec. 2006.

[16] 16 Way Power Divider, Combiner, Splitter. *Available Online* [2017]. http://www.instockwireless.com/16way-power-splitter-combiner-divider-app.htm

[17] R. N. Simons and G. E. Ponchak, "Coax-to-channelised coplanar waveguide in-phase N-way, radial power divider," *Electronics Letters*, vol. 26, no. 11, pp. 754-756, May 1990.

[18] K. W. Eccleston, "N-way microwave power divider using two-dimensional meta-materials," *Electronics Letters*, vol. 42, no. 15, pp. 863-864, July 2006.

[19] H. Chen and Y. X. Zhang, "A novel compact planar six-way power divider using folded and hybrid-expanded coupled lines," *PIER*, vol. 76, pp. 243-252, 2007.

[20] L. I. Parad and R. L. Moynihan, "Split-tee power divider," *IEEE Trans. MTT*, vol. 13, no. 1, pp. 91-95, Jan. 1965.

[21] N-way Wilkinson Divider. Microwave Encyclopedia-Microwaves101.com. *Available Online* [2017]. https://www.microwaves101.com/encyclopedias/n-way-wilkinson-splitters

[22] J.-S. Lim, H.-S. Yang, Y.-T. Lee, S. Kim, K.-S. Seo, and S. Nam, "E-band Wilkinson balun using CPW MMIC technology," *Electronics Letters*, vol. 40, no. 14, pp. 879-880, July 2004.

[23] M.-A. Antoniades and G.-V. Eleftheriades, "A broadband Wilkinson balun using microstrip metamaterial lines," *IEEE Antennas and Wireless Propagation Letters*, vol. 4, no. 1, pp. 209-212, 2005.

[24] Y. Wu, Y. Liu, S. Li, C. Yu, and X. Liu, "Closed-form design method of an N-way dual-band Wilkinson hybrid power divider," *PIER*, vol. 101, pp. 97-114, 2010.

[25] U.-H. Park and J.-S. Lim, "A 700- to 2500-MHz microstrip balun using a Wilkinson divider and 3-dB quadrature couplers," *Microwave and Optical Technology Letters*, vol. 47, no. 4, pp. 333-335, Sept. 2005.

[26] P. Angeletti and M. Lisi, "Multiport power amplifiers for flexible satellite antennas and payloads," *Microwave Journal*, pp. 96-110, May 2010.

[27] B. Ravelo, "Synthesis of N-way active topology for wide-band RF/microwave applications," *International Journal of Electronics*, vol. 99, no. 5, pp. 597-608, May 2012.

[28] O. Maurice, A. Reineix, P. Hoffmann, B. Pecqueux, and P. Pouliguen, "A formalism to compute the electromagnetic compatibility of complex networks," *Advances in Applied Science Research*, vol. 2, no. 5, pp. 439-448, 2011.

[29] S. Lalléchère, B. Ravelo, and A. Thakur, "Statistical performances of resistive active power splitter," *IoP Conf. Ser.: Mater. Sci. Eng.*, vol. 120, no. 1, pp. 12015-12018, 2016.

[30] B. Ravelo, O. Maurice, and S. Lalléchère, "Asymmetrical 1:2 Y-tree interconnects modelling with Kron-Branin formalism," *Electronics Letters*, vol. 52, no. 14, pp. 1215-1216, July 2016.

[31] B. Ravelo and O. Maurice, "Kron-Branin modelling of Y-Y-tree interconnects for the PCB signal integrity analysis," *IEEE Trans. EMC*, vol. 59, no. 2, pp. 411-419, Apr. 2017.

[32] B. Ravelo, O. Maurice, and S. Lalléchère, "Unequal Y-power divider Kron-Branin model," *Proc. of 2017 International Applied Computational Electromagnetics Society (ACES) Symposium*, Suzhou, China, pp. 1-2, 1-4 Aug. 2017.

B. Ravelo holds his Ph.D. degree in 2008 from Univ. Brest and his dissertation to lead research ("HDR= Habilitation à Diriger des Recherches") in 2012 from Univ. Rouen. He is currently Associate Professor at the graduate engineering school ESIGELEC/IRSEEM in Rouen/ France. His research interests cover the microwave circuit design, electromagnetic compatibility (EMC) and interference (EMI), and signal and power integrity (SI/PI) engineering. He is a pioneer of the negative group delay (NGD) RF/analog and digital circuits and systems. He is (co)-author of more than 200 papers and regularly involved in national/international research projects. He co-supervised and directed 9 Ph.D. students whose 6 Ph.D. candidates defended. He is the coordinator of the European TECS Project funded by the program INTERREG VA 4081, he is in charge of the EM characterization of the platform developed in the CareStore Project funded by FP7-SME-2012 and he participates regularly in large R&D international projects. His current publication h-index is 16 (Reference: Google Scholar 2017).

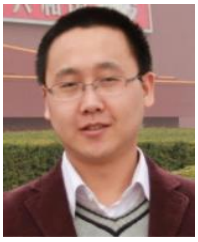

F. Wan received the Ph.D. degree in Electronic Engineering from University of Rouen, Rouen, France, in 2011. From 2011 to 2013, he was a Postdoctoral Fellow in the Electromagnetic Compatibility Laboratory, Missouri University of Science and Technology, Rolla. He is currently a Professor at Nanjing University of Information Science and Technology, Nanjing, China. His current research interests include negative group delay circuit, electrostatic discharge, electromagnetic compatibility, and advanced RF measurement.

S. Lalléchère received the M.Sc. and Ph.D. degrees in Computational Modeling and Electronics from Polytech Clermont and Université Blaise Pascal, Clermont-Ferrand, France, in 2002 and 2006. He is currently an Associate Professor at Université Clermont Auvergne (UCA) and Institut Pascal, Clermont-Ferrand, France. He authored and co-authored more than 120 communications in international journals and conferences. His research interests cover the fields of electromagnetics including electromagnetic compatibility, antennas and propagation, computational electromagnetics, and stochastic modeling in electrical engineering.

Benoit Agnus is the Director of the independent applied research enterprise "Wave Conception." The enterprise is performing research in the areas of electromagnetism, plasmas and multi-parametric servo systems.

Agnus received his Ph.D. in Microwave and Millimeter Wave Engineering Instrumentation and Measurement Techniques in 1994 at the University of Bordeaux 1 in the laboratory of Physics of Interactions Waves Materials ("Physique d'Interaction Ondes Matières = PIOM").

He pursued a 25-year career in industrial Research and Development (R&D) and published several scientific papers. His interest activities are electromagnetic waves, RF/microwave system modeling and post-processing, spatial or terrestrial communication instrumentation, plasma production and control, energy issues for system autonomy, embedded intelligence for the diagnosis and reconfiguration of complex systems, signal processing and RF/microwave transceiver architectures.